01 Nov 1993

An Integrated Surface Seismic/Seismic Profile Case Study: Simonette Area, Alberta

Ronald C. Hinds

Neil Lennart Anderson
Missouri University of Science and Technology, nanders@mst.edu

Richard Kuzmiski

Recommended Citation

R. C. Hinds et al., "An Integrated Surface Seismic/Seismic Profile Case Study: Simonette Area, Alberta," *Geophysics*, vol. 58, no. 11, pp. 1676-1688, Society of Exploration Geophysicists, Nov 1993.
The definitive version is available at https://doi.org/10.1190/1.1443383

GEOPHYSICS, VOL. 58, NO. 11 (NOVEMBER 1993) P. 1676–1688, 16 FIGS.

An integrated surface seismic/seismic profile case study: Simonette area, Alberta

Ronald C. Hinds*, Neil L. Anderson‡, and Richard Kuzmiski**

ABSTRACT

On the basis of conventional surface seismic data, the 13-15-63-25W5M exploratory well was drilled into a low-relief Leduc Formation reef (Devonian Woodbend Group) in the Simonette area, west-central Alberta, Canada. The well was expected to intersect the crest of the reef and encounter about 50–60 m of pay; unfortunately it was drilled into a flank position and abandoned. The decision to abandon the well, as opposed to whipstocking in the direction of the reef crest, was made after the acquisition and interpretive processing of both near- and far-offset (252 and 524 m, respectively) vertical seismic profile (VSP) data, and after the reanalysis of existing surface seismic data.

The near- and far-offset VSPs were run and interpreted while the drill rig remained on-site, with the immediate objectives of: (1) determining an accurate tie between the surface seismic data and the subsurface geology; and (2) mapping relief along the top of the reef over a distance of 150 m from the 13-15 well location in the direction of the adjacent productive 16-16 well (with a view to whipstocking). These surveys proved to be cost-effective in that the operators were able to determine that the crest of the reef was out of the target area, and that whipstocking was not a viable alternative. The use of VSP surveys in this situation allowed the operators to avoid the costs associated with whipstocking, and to feel confident with their decision to abandon the well.

INTRODUCTION

The Upper Devonian Woodbend Group in central Alberta (Figure 1) is subdivided into four formations: Cooking Lake, Duvernay, Leduc, and Ireton. The Cooking Lake (where present) is platform facies, the Leduc is reefal facies, the Duvernay and Ireton are inter-reef shales (Anderson and Brown, 1987; Anderson et al., 1989a and b; Klovan, 1964; Mossop, 1972; Mountjoy, 1980; Stoakes, 1980; Stoakes and Wendte, 1987; and Moore, 1988 and 1989a and b). In the Simonette study area (Figure 2), the Cooking Lake is depositionally absent and the Leduc conformably overlies the Beaverhill Lake Group (Moore, 1989a).

The Leduc in the Simonette study area (Figure 2), developed as both full reef and low-relief reef. The areal extent of the full reef (which towers up to 230 m above the Beaverhill Lake Platform), is defined roughly by the 70 m contour interval of Figure 2. The low-relief reef in contrast, attains a maximum thickness on the order of 120 m; its approximate areal extent is defined by the 130 m contour interval (sections 15, 16, 21, and 22; Figure 2). The updip edges of both types of carbonate buildups can be productive where they are structurally closed and effectively sealed by the inter-reef shales of the Duvernay and Ireton. The geologic cross-section of Figure 3 illustrates the interpreted morphological relationships between the full and low-relief buildups in the Simonette area.

Full reef (Figures 2 and 3) is readily mapped on good quality two-dimensional (2-D) seismic data; it is characterized by appreciable velocity pullup (30 ms), time-structural drape at the top of the Devonian (30 ms), and character variations within the Woodbend interval. The seismic signature of the low-relief reef, as evidenced by the example seismic data (Figure 4), is more subtle, being manifested by less than 15 ms of pullup and less than 15 ms of drape. In addition, the reflection from the top of the low-relief reef can be difficult to distinguish from the *Z*-marker event (a prominent inter-shale event).

In this paper we discuss the 2-D surface seismic and VSP signatures of the low-relief reef in the Simonette study area. The 2-D data (Figure 4) were acquired prior to drilling the 13-15 exploratory well, which ultimately ended up intersect-

Manuscript received by the Editor February 28, 1992; revised manuscript received March 17, 1993.
*Department of Geology, University of Pretoria, Pretoria, South Africa 0002.
‡Kansas Geological Survey, University of Kansas, 1930 Constant Ave., Lawrence, KS 66047.
**Computalog, 600 6th Ave. SW, Calgary, Alberta, Canada T2P 0S5.

ing the reef in a flank position below the oil/water contact. The near- and far-offset VSP surveys were run and processed while the drill rig was still on-site, in an attempt to determine the proximity of the reef crest, and whether 13-15 should have been whipstocked.

SIMONETTE LOW-RELIEF REEF

The edge of the low-relief reef in the Simonette study area is defined roughly by the 130 m contour on the inter-reef shale isopach map (Figure 2). Three wells penetrate this buildup: 16-16-63-25 W5M, 4-22-63-25W5M, and 13-15-63-25W5M. Well 16-16 encountered 72 m of net pay, 4-22 encountered 24 m of net pay but watered out after 12 months of production, and 13-15 is the abandoned exploratory well for which the two VSPs were acquired (Figure 3). This latter well was drilled with the expectation that it would be similar to 16-16.

The contour map of Figure 5 summarizes the geophysical interpretation of the 13-15 location prior to the drilling of the exploratory well. The expectation was that 13-15 would

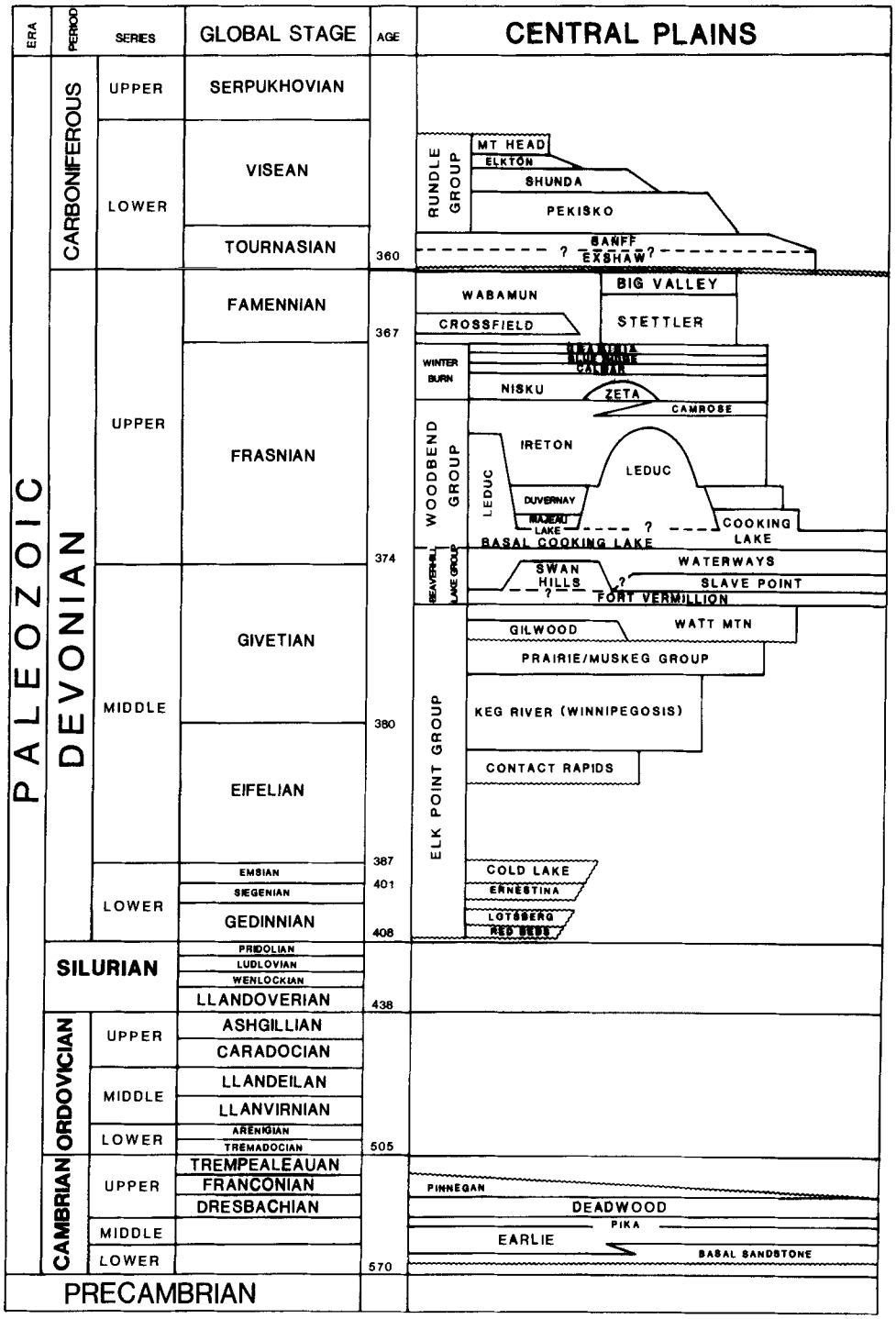

FIG. 1. Stratigraphy of the Central Plains area of the Western Canada Sedimentary Basin (after AGAT Laboratories, 1988).

encounter 50-60 m of net pay. The contour map of Figure 6 summarizes the evaluation of the 13-15 location after drilling, the interpretation of the VSP data, and the reinterpretation of the existing surface seismic coverage.

The surface seismic line (normal polarity display; Figure 4) is nominally 20-fold, split-spread, 120 trace data, acquired using a patterned dynamite source (5 × 2 × 0.5 kg at 9 m) and DFS-V recording equipment (8-128 Hz filter). The groups consisted of nine inline, 14 Hz geophones spaced at 3.75 m. The geophone group, shot, and CMP intervals were 25, 75, and 12.5 m, respectively.

The seismic markers of principal interest are the Mannville, Nordegg, Debolt/Belloy, Wabamun, Ireton, *Z*-marker, and Leduc (Figures 1 and 4). The seismic image of the subsurface at 13-15 (Figure 4) was initially interpreted as comparable to that at the productive 16-16 location; hence 13-15 was drilled. (The high-amplitude event at about 1.9 s, at the 13-15 location, was incorrectly interpreted as the top of the reef. In retrospect, it is believed to be the off-reef *Z*-marker.)

Well 13-15 intersected the low-relief reef in a flank position below the oil/water contact and encountered 134 m of inter-reef shale (in comparison to 75 m of shale encountered in 16-16). On the basis of the 13-15 well results, it was suggested that the low-relief reef could rise abruptly to the west and that whipstocking in the direction of the productive 16-16 well should be considered.

The operators were left with two alternatives: abandon the well or whipstock in the direction of 16-16, bearing in mind that the further 13-15 deviated from the original bottomhole location, the greater the production penalty. To ascertain the cost effectiveness of whipstocking, the operators ran two post-well surveys: a near-offset (252 m) VSP and a far-offset (524 m) VSP. It was on the basis of these data and the reinterpretation of the existing surface seismic that the decision was made to abandon 13-15.

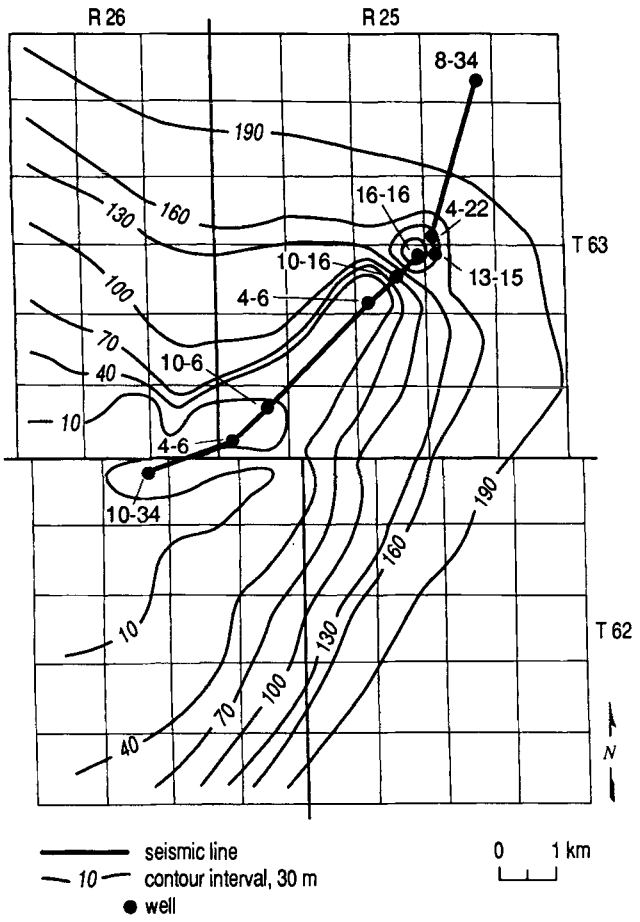

FIG. 2. Inter-reef shale (Ireton/Duvernay) isopach map for the Simonette study area. Contour interval is 30 m. The locations of the eight wells incorporated into the geologic cross-section of Figure 3 and the approximate location of the example seismic line (Figures 4 and 16) are highlighted. The 16-16 well penetrated the crest of the low-relief Leduc reef; 4-22 and 13-15 intersected the flank of the buildup.

VSP ACQUISITION

After the analysis of the 13-15 well logs and prior to abandonment, two VSP surveys were run at this well site to:

1) More accurately tie the surface seismic to the subsurface geology (in particular the top of the low-relief Leduc reef);
2) Map the top of the reef over a distance of 150 m in the direction of the 16-16 well (with a view to whipstocking); and
3) Differentiate primary reflections from both surface-generated and interbed multiples.

The near-offset was 252 m from 13-15, the far-offset was 524 m; both were online with respect to the surface seismic line (Figure 4). Two Vibroseis units were operated at each offset. The 12 s sweep ranged from 10 to 70 Hz, the recording length was 15 s, and the cross-correlated output was 3 s. On average, six sweeps were summed for each geophone sonde location. MDS-10 recording instruments and a sampling interval of 1 ms were used. The recording filter was OUT/250; the instrument filter served as an anti-aliasing, low-pass filter with a ramp rolloff starting at 250 Hz.

Well 13-15 extends 3620 m below the Kelly Bushing (at 878 m asl). Both source locations were at 868 m asl. The geophone sonde was lowered to the bottom of the well and raised at 20–30 m intervals. At each sonde location, the three component geophone tool was locked in place.

NEAR-OFFSET (252 m) VSP INTERPRETIVE PROCESSING

During the processing of the near-offset VSP a series of interpretive processing panels (IPPs) were generated to display the following:

1) Upgoing and downgoing *P*-wave separation;
2) Deconvolution of the separated upgoing *P*-waves using an inverse filter calculated from the separated downgoing *P*-waves; and
3) Inside and outside corridor stacks of both the deconvolved and nondeconvolved upgoing *P*-waves.

Throughout the paper, the abbreviations FRT, −TT time and +TT time (Hinds et al., 1989) are used repeatedly. FRT is the abbreviation for field recorded time, the term used to describe the time-depth display of the raw field records. The terms −TT and +TT refer to specific data configurations.

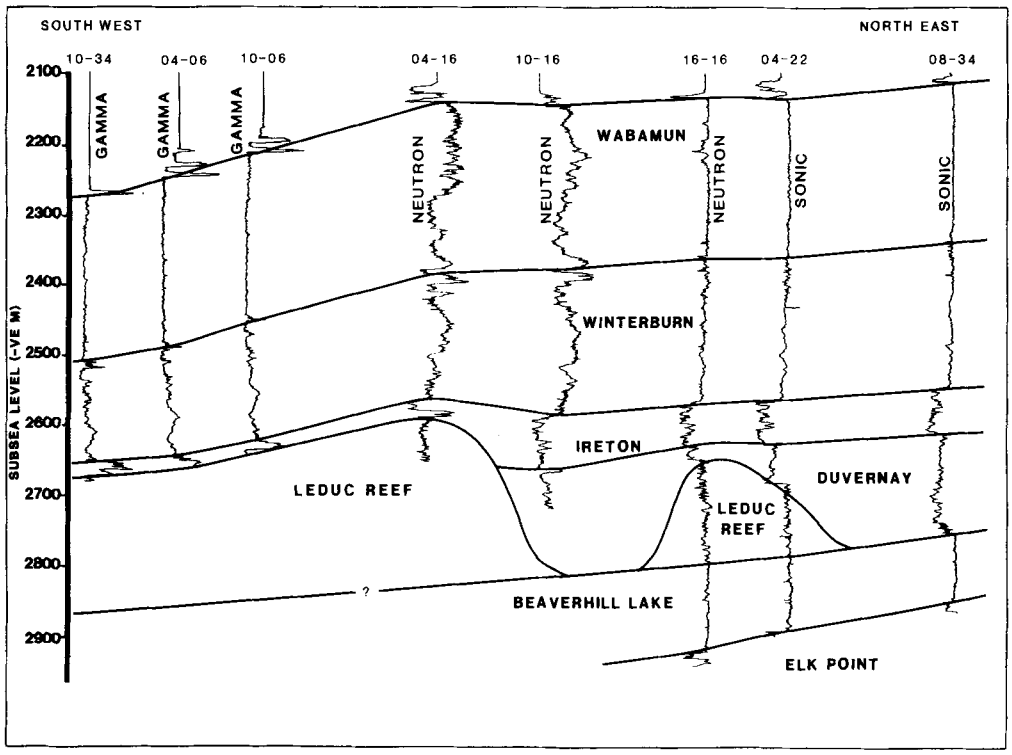

FIG. 3. Geologic section crossing the northeast edge of the Simonette full Leduc reef complex and the adjacent low-relief reef (Figure 2).

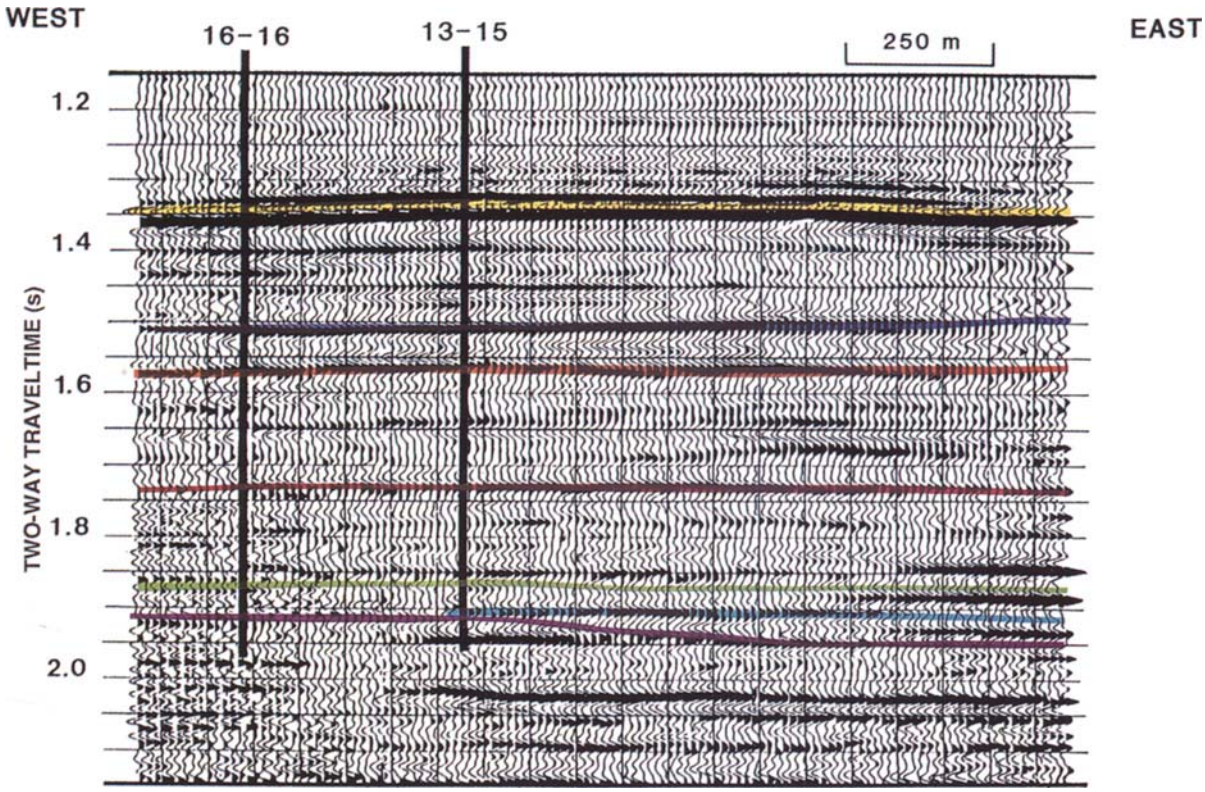

FIG. 4. Example surface seismic section (Figure 5) showing the geophysical interpretation of the 13-15 well site prior to drilling. Drilling and VSP data confirmed that this pre-well interpretation is inaccurate and that the crest of the low-relief reef is west of 13-15. (Mannville-yellow; Nordegg-dark blue; Debolt/Belloy-orange; Wabamun-red; Ireton-green; Z-marker-light blue; Leduc-purple).

−TT is used in reference to the display on which the first breaks and downgoing waves are horizontally aligned and bulk shifted. On these displays, the first-break times have been subtracted from each trace, and the aligned traces have been bulk shifted to an arbitrary time-datum (usually to 100 or 200 ms). +TT is used in reference to the display on which the first-break time of each trace has been added to that trace [plus possible normal moveout (NMO) corrections]. On the +TT displays, the upgoing waves are aligned and should be in pseudo two-way traveltime. Unless otherwise noted, the VSP data displays are normal polarity. For clarity, only every second trace is plotted on most of the VSP displays.

P-wave separation

The separation of the upgoing and downgoing *P*-waves on the vertical (*Z*) geophone data is illustrated in the wavefield separation IPP (Figure 7).

Panel 1 (Figure 7) display the Z data after gain adjustment. In panel 2, high-amplitude surface-generated multiples, and less prominent interbed multiples are shown. The surface-generated downgoing multiples can be recognized as continuous events arriving after the first-break primary downgoing wave train on all of the traces, from the deepest to the shallowest receiver location. If the downgoing multiple does not extend over the entire depth range (present on deeper receiver location traces only) it is an interbed multiple (Hinds et al., 1989). For example, a downgoing Mannville interbed multiple is interpreted to start at the 2080 m trace (between 0.3 and 0.32 s; panel 2) and continue onto the deeper traces.

The downgoing waves were separated from the combined wavefields using an eleven-point median filter (panel 3). The residual upgoing wave content in panel 4 is minimal. The upgoing waves (panel 4) were separated from the combined wavefield (panel 2) by effectively subtracting the downgoing wavefield (panel 3) using median filters (Balch and Lee, 1984; Hardage, 1985; Hinds et al., 1989). The Mannville, Nordegg, Belloy/Debolt, Wabamun, Ireton, Z-marker, and reefal Leduc events are interpreted in the median filtered upgoing wavefield (panel 5; Figure 7).

Near-offset VSP deconvolution

Multiple reflections are represented in the downgoing wavefield (panel 3; Figure 7). The initial downgoing pulse (except in the case of head wave contamination) is the primary downgoing *P*-wave; later downgoing arrivals are multiples. These multiples can be effectively removed by deconvolving the upgoing wave data with an inverse filter derived from an analysis of the downgoing wave train (Hinds et al., 1989). The IPP of Figure 8 enables the interpreter to monitor deconvolution. The first panel of Figure 8 is the median-filtered, separated, nondeconvolved upgoing wavefield. Panels 2 and 3 are the combined wavefield and separated downgoing wavefield, respectively. Panel 4 is the deconvolved upgoing wavefield.

Panel 5 is the median filtered, deconvolved upgoing wavefield. A comparison of the first panel (Figure 8) with the last, illustrates the effect of the multiple contamination on the continuity of primary events. In panel 1 for example, the Debolt/Belloy event is high amplitude and continuous at

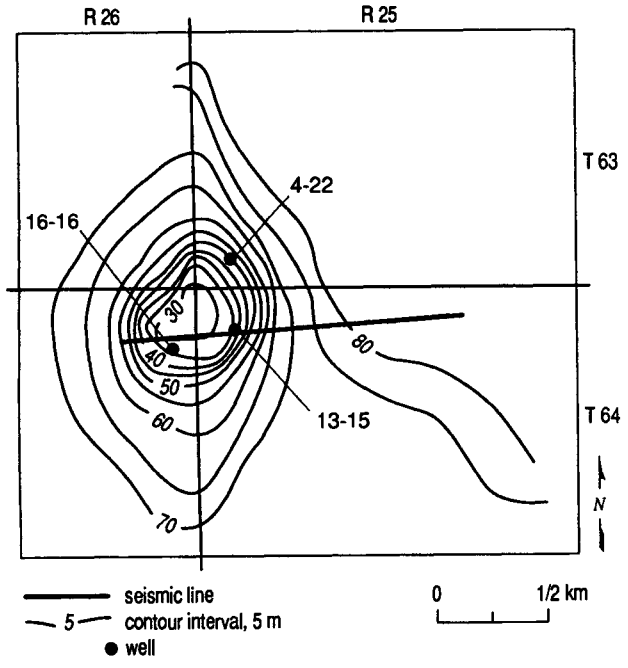

FIG. 5. Inter-reef shale isochron map illustrating the interpretation of the 13-15 well site prior to drilling. Contour interval is 10 ms. 13-15 was expected to encounter about 75 m (about 35 ms) of inter-reef shale and productive Leduc reef. Unfortunately 13-15 penetrated 136 m (about 63 ms) of inter-reef shale and wet Leduc. Seismic control in addition to the example line shown (Figure 4) was used to construct this map.

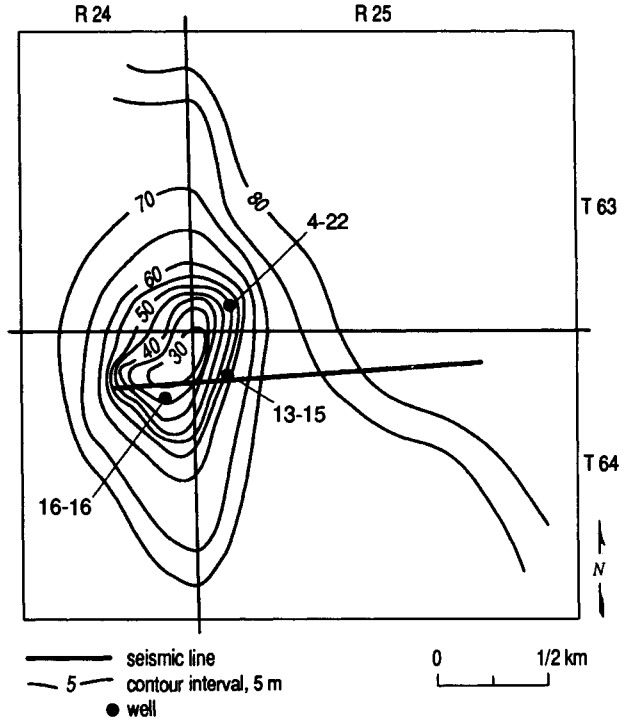

FIG. 6. Inter-reef shale isochron map (in ms) illustrating the revised interpretation of the 13-15 well site. Drilling and VSP data confirmed that the crest of the low-relief reef (as demarcated by the 40 ms contour interval) is west of 13-15.

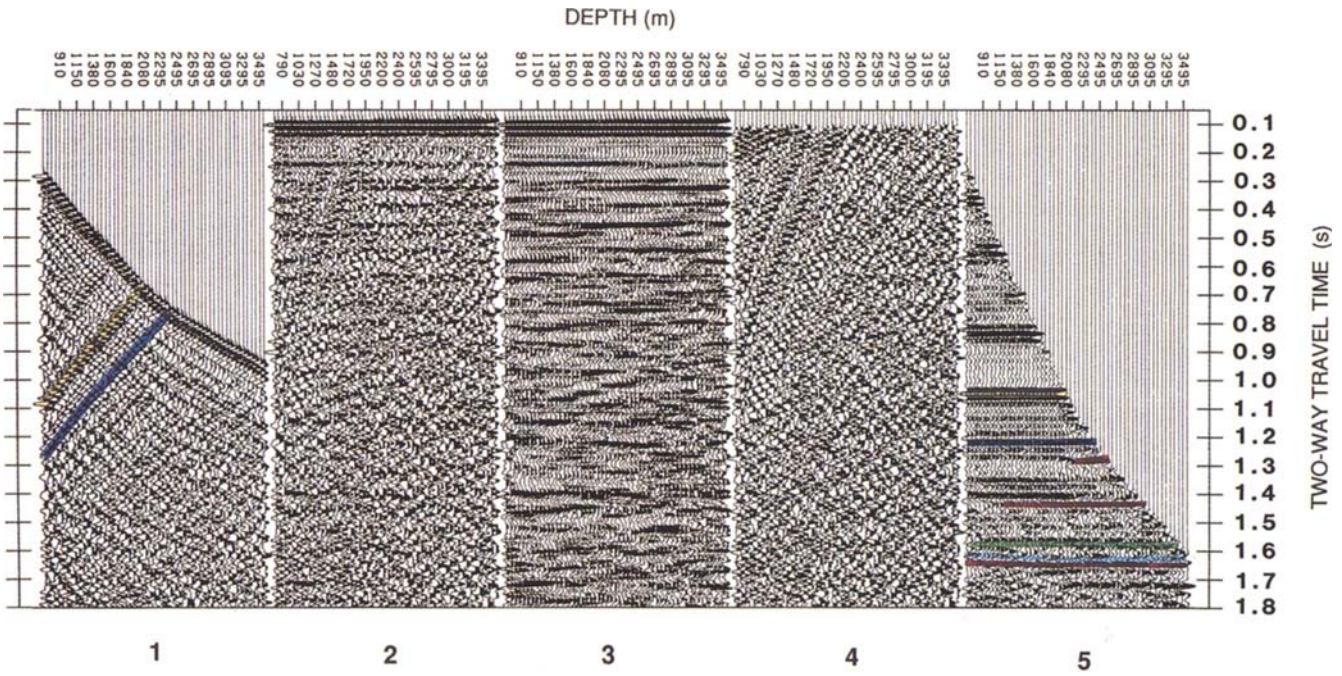

FIG. 7. Interpretive processing panel depicting the wavefield separation of the near-offset VSP. [1: gained raw data (FRT); 2: gained raw data (−TT); 3: separated downgoing waves (−TT); 4: separated upgoing waves (−TT); 5: median filtered upgoing waves (+TT)]. (Mannville-yellow; Nordegg-dark blue; Debolt/Belloy-orange; Wabamun-red; Ireton-green; Z-marker-light blue; Leduc-purple).

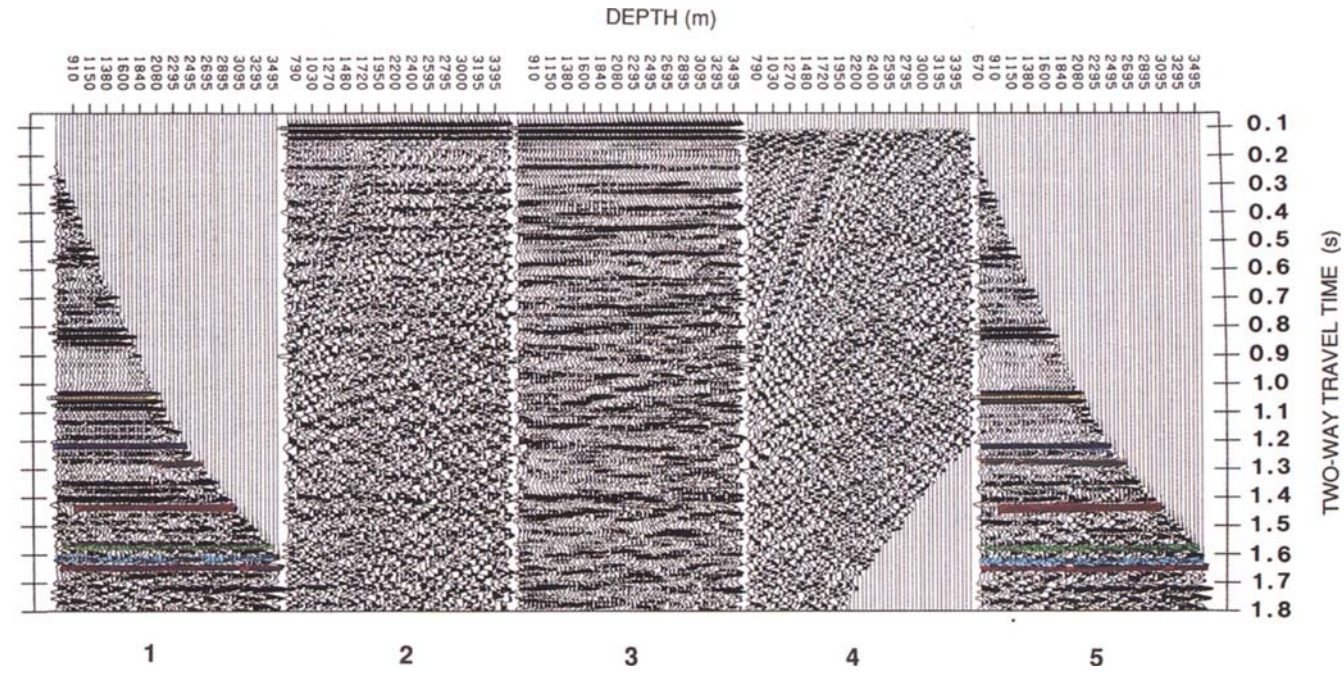

FIG. 8. Interpretive processing panel depicting the deconvolution of the near-offset VSP. [1: median filtered upgoing waves (+TT); 2: separated downgoing waves (−TT); 3: separated upgoing waves (−TT); 4: deconvolved, separated upgoing waves (−TT); 5: median filtered, deconvolved, upgoing waves (+TT)]. (Mannville-yellow; Nordegg-dark blue; Debolt/Belloy-orange; Wabamun-red; Ireton-green; Z-marker-light blue; Leduc-purple).

sonde depths below the top of the Mannville (2080 to 2570 m). At shallower recording depths, the Debolt/Belloy event and a Mannville interbed multiple interfere. On panel 5, deconvolution appears to have substantially reduced the effect of multiple interference.

Within the zone of interest (Wabamun to Leduc), multiple contamination appears to be minimal. The Z-marker and Leduc events are continuous and do not exhibit either significant apparent time-structural relief or appreciable character variations.

Inside and outside corridor stacks

Multiple contamination of upgoing waves can be re-examined using inside and outside corridor stacks. Nondeconvolved inside corridor stacks contain both primary and multiple events; nondeconvolved outside corridor stacks should be relatively free of multiples. If deconvolution is successful in removing multiples, then inside and outside corridor stacks of deconvolved data will be predominated by primary reflections.

Nondeconvolved, inside and outside corridor stacks along with the input data to the muting and stacking processes are shown in Figure 9. On the nondeconvolved inside corridor stack (panel 4; Figure 9), the amplitude of the Debolt/Belloy is weak compared to this event on the outside corridor stack (panel 3). On the muted input data (panel 5) for the nondeconvolved inside corridor stack, the Debolt/Belloy event at sonde depths shallower than the Mannville (approximately 2080 m), is masked by an interbed multiple. At sonde depths greater than the Mannville, the Debolt/Belloy event is higher amplitude and 5–10 ms deeper.

On the outside and inside deconvolved corridor stacks (panels 3 and 4; Figure 10), the interbed multiples and surface-generated multiples appear to have been substantially attenuated by deconvolution. Short period, interbed multiples have been attenuated but not totally removed. As is the case with surface seismic processing, as the period of the interbed multiple shortens, successful deconvolution becomes increasingly difficult.

FAR-OFFSET (524 m) VSP INTERPRETIVE PROCESSING

The vertical (Z) and horizontal (X and Y) axis on the far-offset VSP data, contain nonpartitioned elements of the upgoing and downgoing *P*- and *SV*-wavefields. An examination of the far-offset IPPs reveals that wavefield partitioning has significant implications with respect to the interpretation of these data.

Hodogram-based rotation

The X, Y, and Z channel data are presented in Figure 11 as panels 1, 2, and 3, respectively. The hodogram-based method initially polarized the components of the X and Y data onto HMIN and HMAX axes (Hinds et al., 1989). HMAX axis is horizontally aligned in a plane defined by the source and wellbore. HMIN (panel 4) is also in the horizontal plane but orthogonal to the plane defined by the source and wellbore. As evidenced by panel 5, HMAX data display consistent primary downgoing *P*-wave first breaks, indicating that the first set of rotations was relatively successful.

The Z and HMAX data were input to a second rotation that polarized on downgoing *P*-waves (assuming that the upgoing *P*-wave raypaths is orthogonal to the calculated axis projection). The Z axis was rotated to near horizontal (Z′); HMAX was rotated to a near-vertical position (HMAX′). The downgoing *P*-waves were effectively polarized onto the HMAX′ axis.

Z′ data (panel 6) contain the downgoing shear-wave primaries and multiples, and some upgoing *P*-waves. Note for example, the downgoing Mannville mode-converted *SV*-wave and the trailing downgoing *SV*-multiples. In more detail, the Mannville mode-converted downgoing *SV*-wave primary (at 0.68 s on 2080 m trace; panel 6) can be traced down to 1.12 s on the 3570 m trace (with a greater slope than the downgoing *P*-wave). Two visible, downgoing *SV*-multiples parallel the primary and arrive within a 150 ms window on the 3570 m trace.

On HMAX′ data (panel 7), downgoing *P*-wave energy is predominant. (Note that the rotation required to isolate the downgoing *P*-wave data onto a single panel (HMAX′) has not isolated the upgoing *P*-wave data.)

Time-variant, model-based rotation

In the first stage of the time-variant model-based rotation, Z′ and HMAX′ data were wavefield separated (using frequency wavenumber filtering) into $HMAX'_{down}$, $HMAX'_{up}$, Z'_{down} and Z'_{up}. (The subscripts "up" and "down" denote upgoing and downgoing wavefields, respectively.)

To remove the effects of the previously applied Z to Z′, and HMAX to HMAX′ transformations (necessary to isolate the downgoing *P*-waves), the Z'_{up} and $HMAX'_{up}$ (panels 1 and 2 in Figure 12, respectively) were derotated (using the inverse operation of the previous polarization rotation). The output data of the derotation process, namely the $HMAX_{up(derot)}$ and $Z_{up(derot)}$ are shown as panels 3 and 4 (Figure 12), respectively. Most of the upgoing *P*-wavefield has been distributed back onto the Z-type axis, $Z_{up(derot)}$. Unlike the raw Z data (panel 2; Figure 11), where the downgoing *P*-waves were predominant, the separated upgoing *P*-wave events in the $Z_{up(derot)}$ data are dominant and interpretable.

The upgoing *P*-wave events on the $Z_{up(derot)}$ data (panel 4) are improperly aligned (particularly those generated by shallow reflectors) because of the choice of rotation angles. These data have been derotated but the upgoing *P*-wave events are still partitioned on both output data sets ($Z_{up(derot)}$ and $HMAX_{up(derot)}$) because of the nonzero source offset. The deeper events do not suffer much misalignment because deep event raypath geometries satisfy the near-vertical incidence angle assumption better than the raypaths of shallow events.

To correct for misalignment, time-variant rotation angles were calculated (using paraxial ray tracking; Beydoun, 1985, personal communication) and applied to every pair of traces in panels 3 and 4. The output $HMAX''_{up}$ (panel 5) contains the predominant distribution of the downgoing remnant *SV*-wave data. Z''_{up} (panel 6) contains the predominant distribution of the upgoing *P*-waves. On Z''_{up}, shallow events (originating at 0.58 s between the traces for 1630 to 1750 m) appear to be better aligned than on the $HMAX'_{up}$ data (panel 5).

(text continued on p. 1687)

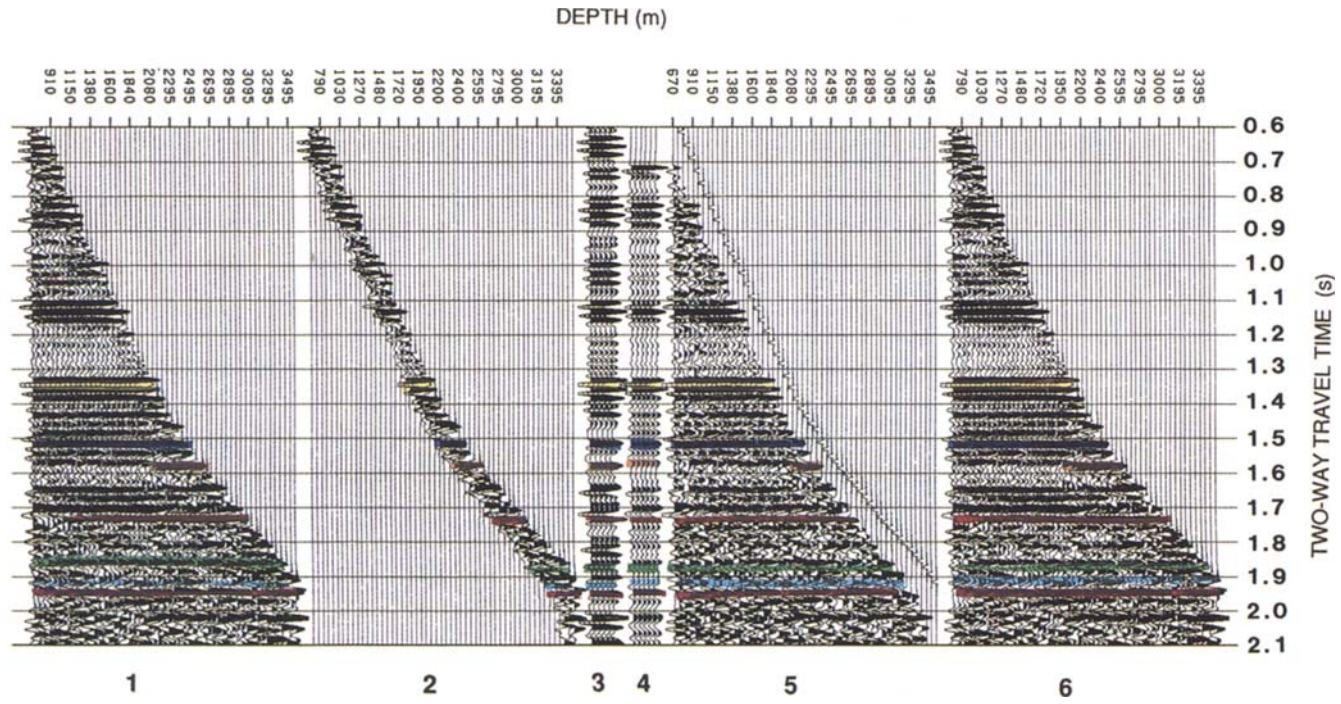

FIG. 9. Interpretive processing panel illustrating the utility of nondeconvolved inside and outside corridor stacks. [1 and 6: median filtered upgoing waves (+TT); 2: muted outside corridor data (+TT); 3: outside corridor stack (+TT); 4: inside corridor stack (+TT); 5: muted inside corridor data (+TT)]. (Mannville-yellow; Nordegg-dark blue; Debolt/Belloy-orange; Wabamun-red; Ireton-green; Z-marker-light blue; Leduc-purple).

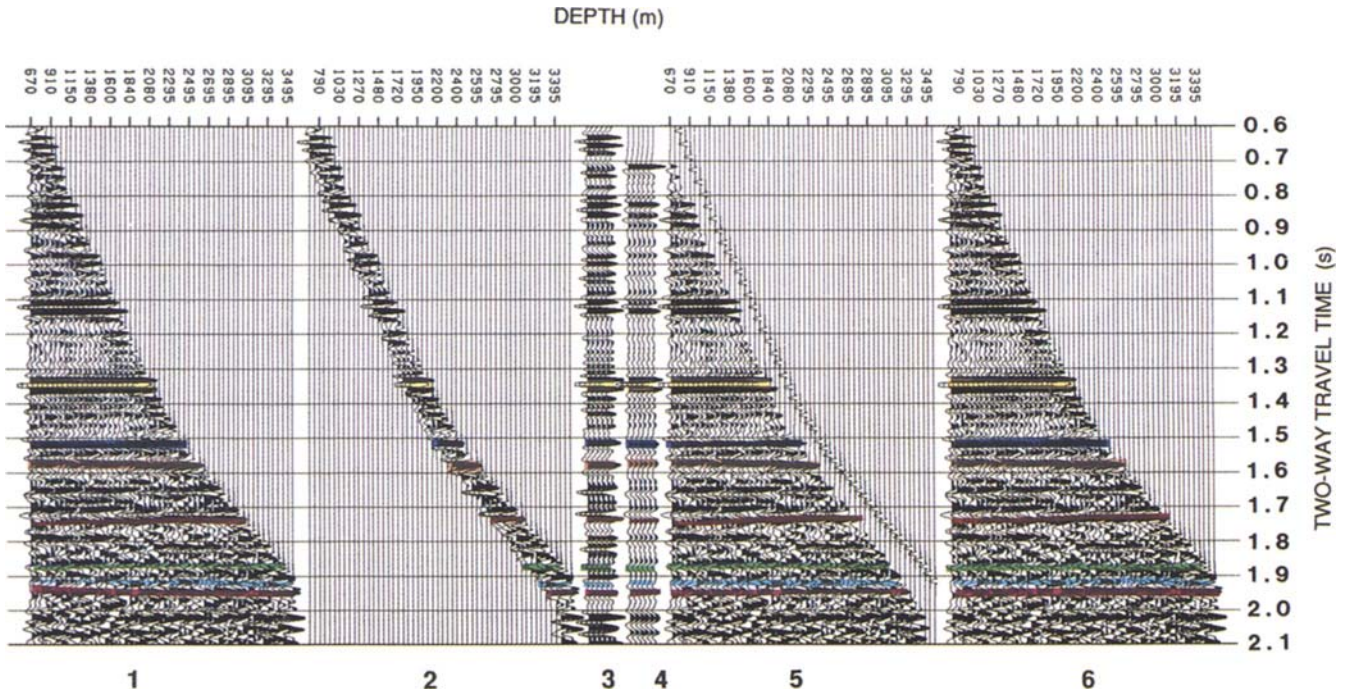

FIG. 10. Interpretive processing panel illustrating the utility of deconvolved inside and outside corridor stacks. [1 and 6: median filtered upgoing waves (+TT); 2: muted outside corridor data (+TT); 3: outside corridor stack (+TT); 4: inside corridor stack (+TT); 5: muted inside corridor data (+TT)]. (Mannville-yellow; Nordegg-dark blue; Debolt/Belloy-orange; Wabamun-red; Ireton-green; Z-marker-light blue; Leduc-purple).

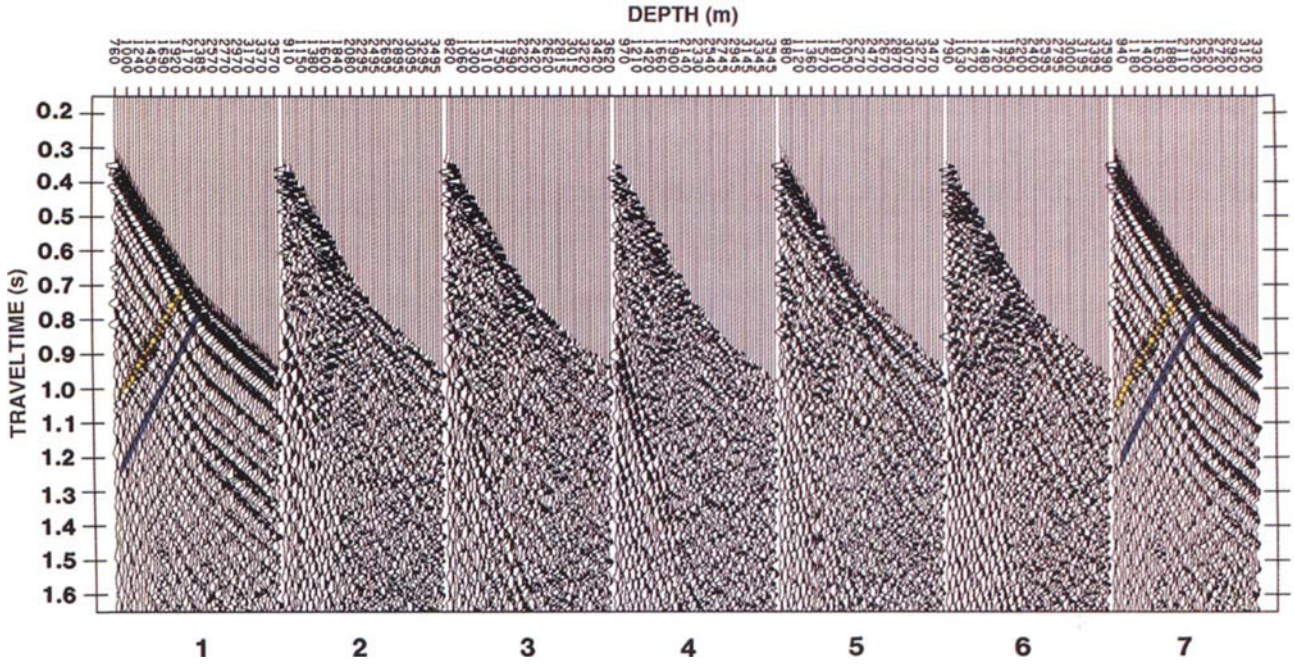

FIG. 11. Interpretive processing panel depicting the hodogram-based data rotation of the far-offset VSP. [1: X-axis data (FRT); 2: Y-axis data (FRT); 3: Z-axis data (FRT); 4: HMIN data (FRT); 5: HMAX data (FRT); 6: Z′-axis data (FRT); 7: HMAX′ data (FRT)]. (Mannville-yellow; Nordegg-dark blue; Debolt/Belloy-orange; Wabamun-red; Ireton-green; Z-marker-light blue; Leduc-purple).

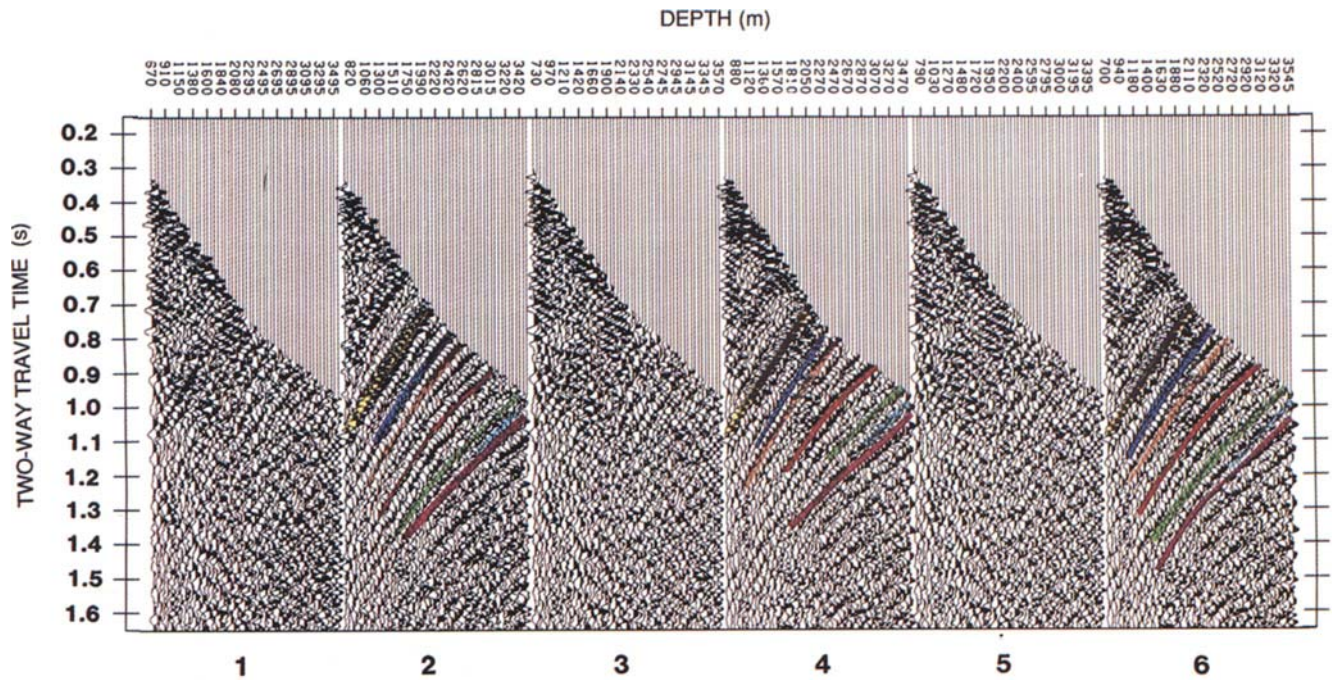

FIG. 12. Interpretive processing panel depicting the time-variant model-based rotation of the far-offset VSP. Note that panels 4 and 6 are opposite polarity due to the extreme derotation angles. [1: Z'_{up} data (FRT); 2: $HMAX'_{up}$ data (FRT); 3: $HMAX_{up(derot)}$ data (FRT); 4: $Z_{up(derot)}$ data (FRT); 5: $HNAX''_{up}$ data (FRT); 6: Z''_{up} data (FRT)]. (Mannville-yellow; Nordegg-dark blue; Debolt/Belloy-orange; Wabamun-red; Ireton-green; Z-marker-light blue; Leduc-purple).

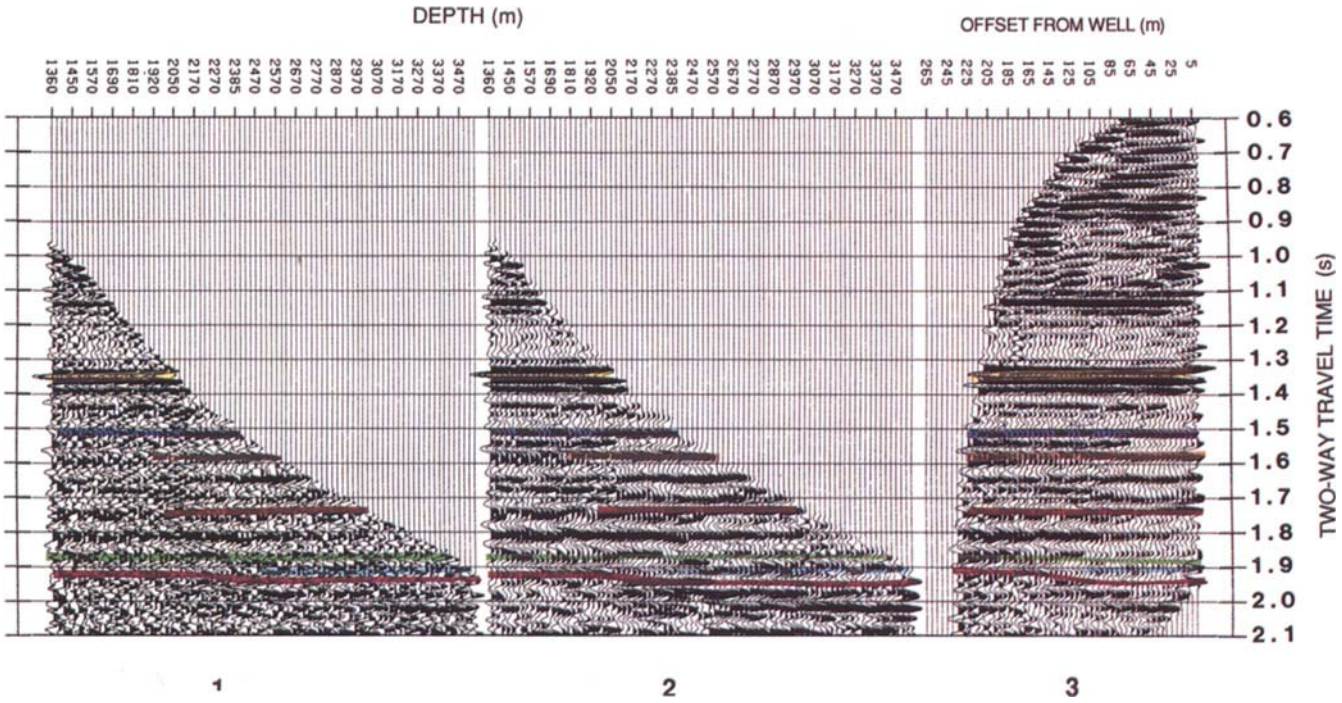

FIG. 13. Interpretive processing panel showing the VSP-CDP transformation of the nondeconvolved far-offset VSP data. [1: Z''_{up} data (FRT); 2: median filtered Z''_{up} data (FRT); 3: median filtered Z''_{up} VSP-CDP data (FRT)]. (Mannville-yellow; Nordegg-dark blue; Debolt/Belloy-orange; Wabamun-red; Ireton-green; Z-marker-light blue; Leduc-purple).

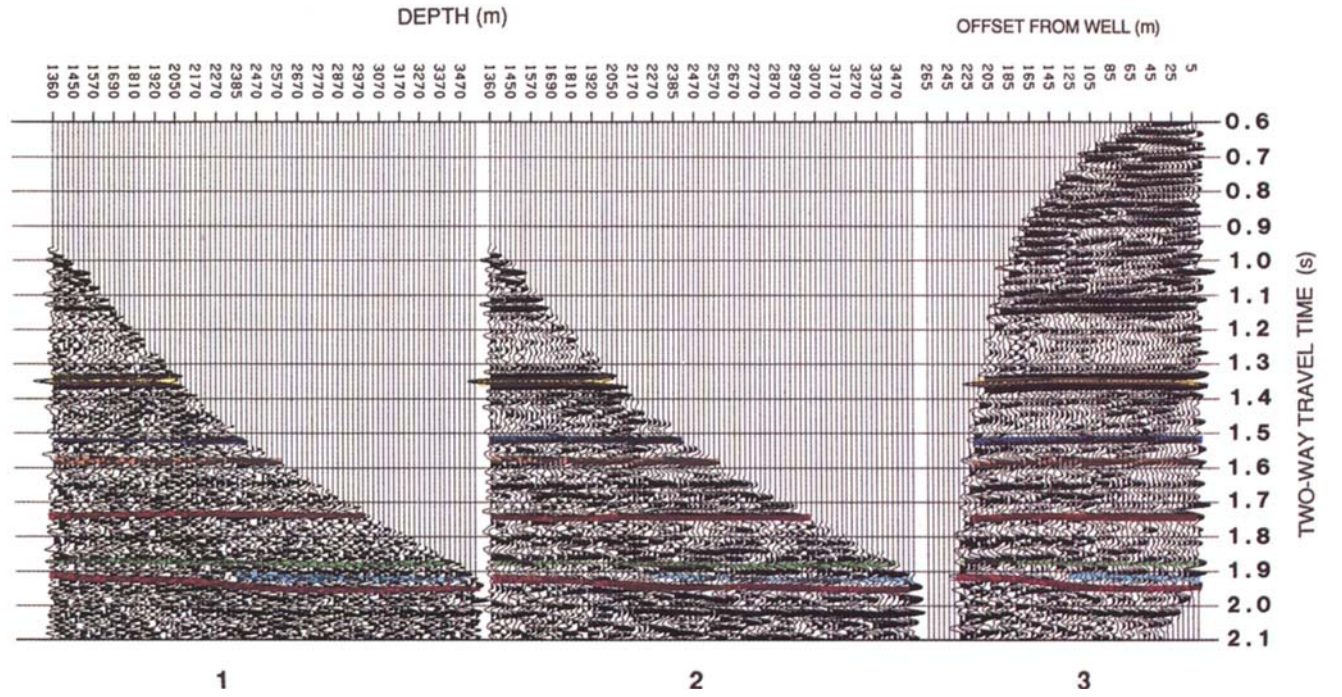

FIG. 14. Interpretive processing panel showing the VSP-CDP transformation of the deconvolved far-offset VSP data. [1: Z''_{up} data (FRT); 2: median filtered Z''_{up} data (FRT); 3: median filtered Z''_{up} VSP-CDP data (FRT)]. (Mannville-yellow; Nordegg-dark blue; Debolt/Belloy-orange; Wabamun-red; Ireton-green; Z-marker-light blue; Leduc-purple).

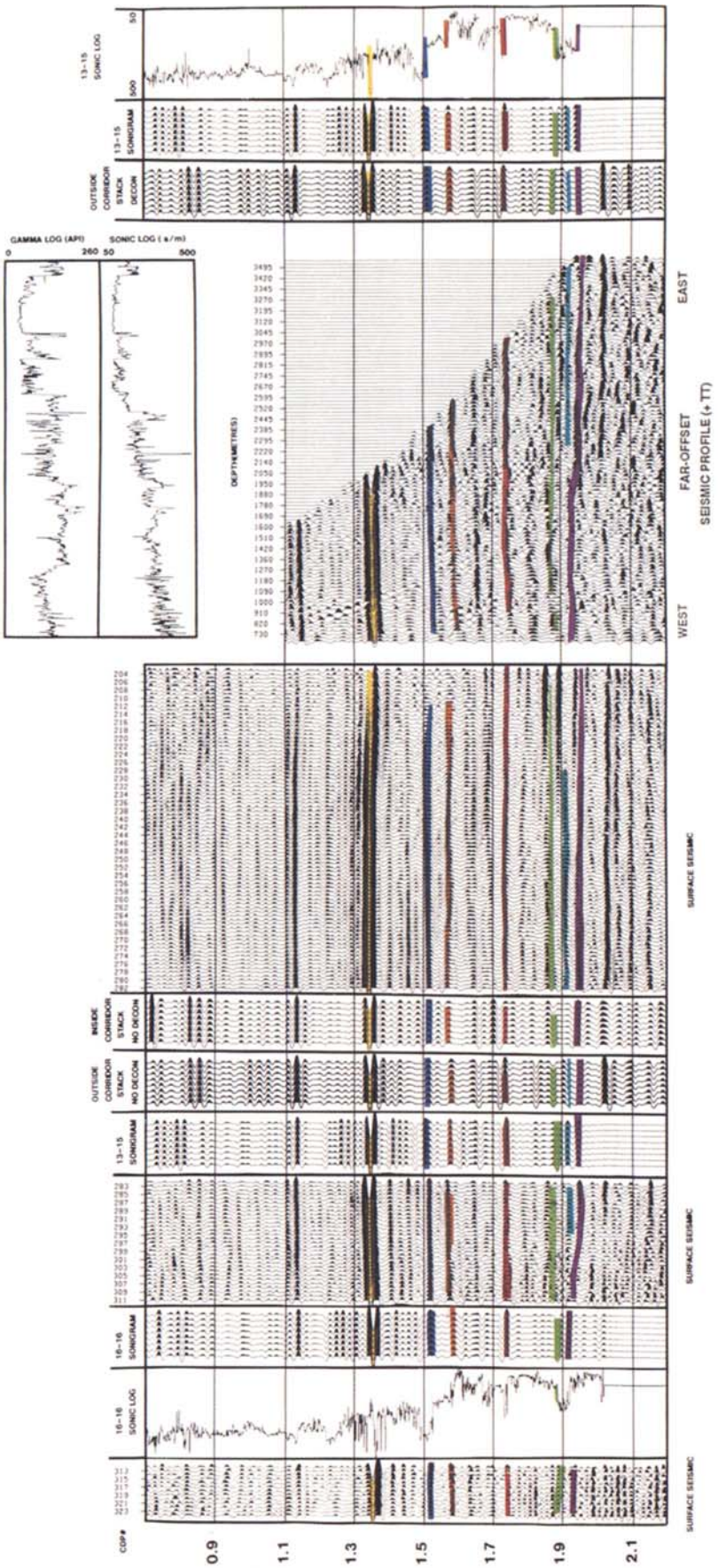

FIG. 15. Integrated interpretive display showing the interpretation of the near- and far-offset data, the surface seismic line, and additional relevant exploration control. (Mannville-yellow; Nordegg-dark blue; Debolt/Belloy-orange;Wabamun-red; Ireton-green; Z-marker-light blue; Leduc-purple).

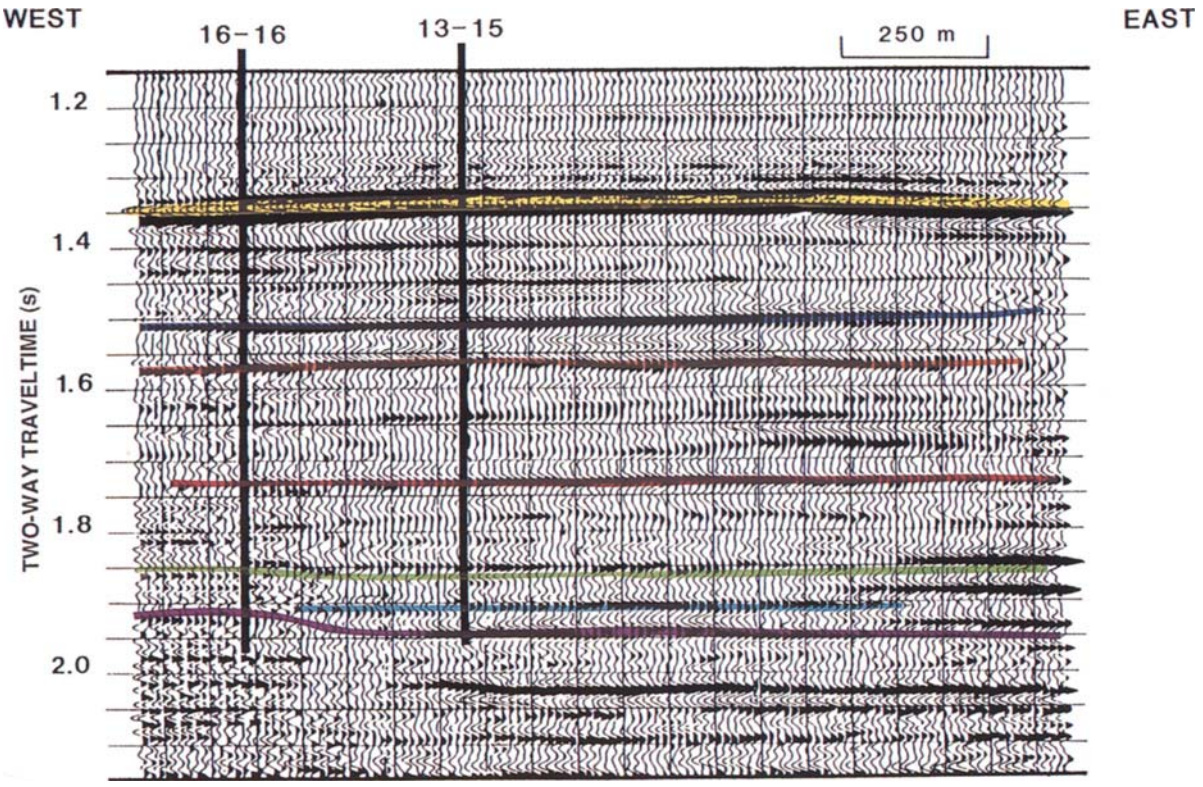

FIG. 16. Revised (post-well) interpretation of the example seismic line (Figure 4). This interpretation is consistent with the 13-15 well information and the VSP data. (Mannville-yellow; Nordegg-dark blue; Debolt/Belloy-orange; Wabamun-red; Ireton-green; Z-marker-light blue; Leduc-purple).

VSP-CDP transformation of the far-offset VSP data

The Z''_{up} data (panel 2; Figure 13) were used for the interpretation of the low-relief Leduc reef. Because of the relatively small offset of the source (524 m) in comparison to the overall depth of the borehole, VSP deconvolution was attempted on the Z''_{up} data. Nonmedian filtered, median filtered, and VSP-CDP transformed (Dillon and Thomson, 1984), nondeconvolved and deconvolved data are displayed in Figures 13 and 14, respectively.

The nondeconvolved VSP-CDP data (Figure 13) show Mannville interbed multiples interfering with deeper *P*-wave primaries. Significant multiple contamination is interpreted between the shallowest trace and the 2080 m trace (top Mannville), and is perhaps best illustrated by the Debolt/Belloy event (panel 2; Figure 13). This horizontally aligned, upgoing primary event (at 1.58 s) is a high amplitude peak at sonde depths greater than 2080 m. At shallower depths, the Debolt/Belloy primary is degraded by the Mannville multiple. In panel 2 of Figure 14, deconvolution has enhanced the Debolt/Belloy event in this shallow sonde interval.

Panel 3 in both Figures 13 and 14 displays the VSP-CDP transformed traces. The Mannville, Nordegg, Debolt/Belloy, Wabamun, Ireton, Z-marker, and Leduc events are correlated. Possible Debolt/Belloy multiples are interpreted within the zone of interest (Ireton/Leduc interval). Panels 1 and 2 (Figure 13) display an Ireton event that appears to truncate abruptly (extending from the deepest trace to the trace below the Debolt/Belloy event). The deconvolved Ireton event (panels 1 and 2; Figure 14) is relatively free of this interpreted multiple interference.

Reefal and associated structure is interpreted on the VSP-CDP displays. The Z-marker (Panel 3; Figure 14) rises gradually to the west of 13-15. The reef top, although less discernable, also rises gradually away from the wellbore; at about 120 m, the reflection from the top of the reef visually merges with the Z-marker event.

INTEGRATED INTERPRETATION

On the left-hand side of the integrated interpretive display (Figure 15), sonic logs for 16-16 and 13-15, nondeconvolved, near-offset, inside and outside corridor stacks are time-tied to the post-VSP (vertical seismic profiling) interpretation of the surface seismic data. On the right-hand side, the far-offset VSP is time-tied to both the 13-15 sonic log, and the deconvolved, near-offset, outside corridor stacks. The horizontal (depth axis) of the far-offset VSP corresponds to the same scale used for the 13-15 sonic and gamma ray log depth display.

The correlated data (Figure 15) allow for the confident interpretation of the surface seismic line and the identification of the Mannville, Nordegg, Debolt/Belloy, Wabamun, Ireton, Z-marker, and Leduc events. Note that within the inter-reef shale interval, the sonic log-based synthetic seismogram is a poor fit to the VSP and surface seismic, and

exhibits up to a 5 ms mistie. The sonic measurements could be at fault in that wellbore effects such as washouts, or the increased concentration of heavy drilling fluids injected into the borehole (intended to prevent a blowout) could have changed the sonic character of strata in the vicinity of the wellbore. Alternatively, these misties could be related to wavelet variability or phase problems with the data. Whatever the source, such discrepencies between sonic log based synthetic seismograms and seismic data provide additional justification for acquiring seismic profile data.

The post-VSP version of the surface seismic section (normal polarity display; Figure 16) differs slightly from the pre-well interpretation (Figure 4) in several respects. Of particular significance is that on the updated version, the Z-marker is present at the 13-15 location, indicating that the well is situated in a flank position. The reinterpreted surface seismic line shows an interpretation of a flat reef extending out from the borehole 100–120 m. This is in agreement with the interpreted near- and far-offset VSP data. Beyond the coverage of the VSP, the reef crests. With respect to lateral variations in the thickness of the inter-reef shale isochron (shale thinning is indicative of reefal thickening) the following interpretations can be made:

1) The shale is 136 m thick (63 ms) on the trace nearest the 13-15 well;
2) The shale is 120 m thick (55 ms) at distances on the order of 100 m from the well; and
3) The shale is 102 m thick (47 ms) at traces representing distances of around 150 m from the well.

On the basis of the reinterpreted surface seismic and VSP data, a revised post-VSP inter-reef shale isochron map (incorporating available well and surface seismic data) was drafted (Figure 6). This map locates the 13-15 exploratory well in a reef flank position, and indicates that the crest of the low-relief reef is in excess of 150 m to the west of 13-15.

SUMMARY

The 13-15-63-25W5M exploratory well was drilled into low-relief Leduc reef in the Simonette area, Alberta. The well was expected to intersect the crest of the reef and to encounter 50–60 m of pay. Unfortunately, it was drilled into a flank position and ultimately abandoned. The decision to abandon the well, as opposed to whipstocking, was made after the acquisition and interpretive processing of the near- and far-offset VSP data, and after the reanalysis of existing surface seismic data. The VSP data were acquired and interpreted while the drill rig remained on-site, awaiting the decision to whipstock or abandon.

On the basis of the VSP data the operators were able to: (1) determine an accurate tie between the surface seismic data (Figure 16) and the subsurface geology, and identify a mistie between the surface seismic and sonic log seismogram; (2) determine that the reef crest was not close enough to 13-15 to make whipstocking a viable option given the production penalties involved in drilling out of the target area; and (3) identify surface-generated and interbed multiples, and ascertain their effect on the surface seismic.

ACKNOWLEDGMENTS

BP Resources Canada Ltd. generously authorized the publication of their proprietary seismic data. Computalog Ltd. of Calgary provided access to the Halliburton Geophysical Inc. VSP processing system; BP Resources Canada Ltd., Inverse Theory and Application Inc., Anglo-American Prospecting Services, and the University of Pretoria allowed us to use their respective seismic data processing systems. Partial support was provided by the National Geophysics Program of South Africa. Our thanks are also extended to Professor P. G. (Pat) Eriksson; his constructive criticisms were appreciated.

REFERENCES

AGAT Laboratories, 1988, Table of formations of Alberta: AGAT Laboratories, Calgary.

Anderson, N. L., and Brown, R. J., 1987, The seismic signatures of some western Canadian Devonian reefs: J. Can. Soc. Expl. Geophys., **23**, 7–26.

Anderson, N. L., Brown, R. J., and Hinds, R. C., 1989a, Low- and high-relief Leduc Formation reefs: A seismic analysis: Geophysics, **54**, 1410–1419.

Anderson, N. L., White, D., and Hinds, R. C., 1989b, Woodbend Group reservoirs, *in* Anderson, N. L., Hills, L. V., and Cederwall, D. A., Eds., Geophysical atlas of western Canadian hydrocarbon pools: Can. Soc. Expl. Geophys./Can. Soc. Petr. Geol., 101–132.

Balch, A. H., and Lee, M. W., 1984, Vertical seismic profiling-techniques, applications and case histories: Int. Human Res. Devel. Corp.

Dillon, P. B., and Thomson, R. C., 1984, Offset source VSP surveys and their image reconstruction: Geophys. Prosp., **32**, 790–811.

Hardage, B. A., 1985, Vertical seismic profiling: Geophys. Press, 2nd edition.

Hinds, R. C., Kuzmiski, R. K., Botha, W. J., and Anderson, N. L., 1989, Vertical and lateral seismic profiles, *in* Anderson, N. L., Hills, L. V., and Cederwall, D. A., Eds., Geophysical atlas of western Canadian hydrocarbon pools: Can. Soc. Expl. Geophys./ Can. Soc. Petr. Geol., 319–344.

Klovan, J. E., 1964, Facies analysis of the Redwater reef complex, Alberta, Canada: Bull. Can. Petr. Geol., **12**, 2260–2281.

Moore, P. F., 1988, Devonian geohistory of the western interior of Canada, *in* McMillan, N. J., Embry, A. F., and Glass, D. J., Eds., Devonian of the World: Can. Soc. Petr. Geol., Memoir 14, 67–87.

——— 1989a, Devonian reefs in Canada and some adjacent areas, *in* Geldsetzer, H. H. J., James, N. P., and Tebbutt, G. E., Eds., Reefs, Canada and Adjacent areas: Can. Soc. Petr. Geol., Memoir 13, 367–390.

——— 1989b, The Kaskaskia Sequence: Reefs, platforms, and foredeeps, The lower Kaskaskia Sequence—Devonian, *in* Ricketts, B. D., Eds., Western Canada sedimentary basin, a case history: Can. Petr. Geol., 139–164.

Mossop, G. D., 1972, Origin of the peripheral rim, Redwater reef, Alberta: Bull. Can. Petr. Geol., **20**, 238–280.

Mountjoy, E., 1980, Some questions about the development of Upper Devonian carbonate buildups (reefs), Western Canada: Bull. Can. Petr. Geol., **28**, 315–344.

Stoakes, F. A., 1980, Nature and control of shale basin fill and its effect on reef growth and termination: Upper Devonian Duvernay and Ireton Formations of Alberta, Canada: Bull. Can. Petr. Geol., **28**, 345–410.

Stoakes, F. A., and Wendte, J. C., 1987, The Woodbend Group, *in* Krause, F. F., and Burrows, O. G., Eds., Devonian lithofacies and reservoir styles in Alberta: Second International Symposium Devonian System, 153–170.